Phasing a sparse telescope

Erez N. Ribak, B. M. Levine and E. Behar

Department of Physics, Technion - Israel Institute of Technology

ABSTRACT

We designed and built a laboratory model of a sparse space telescope. The purpose of the model is to test various algorithmic, optical, and mechanical issues with such a telescope: how to achieve alignment after deployment that yields diffraction limited optical performance. Our model uses four non-redundant sparse sectors. Each segment has three degrees of freedom, with supplementary coarse focusing, so the search volume for a perfect image is quite large, ~10^{51}. We tried stochastic searches, optimizing the point spread to its minimum, and are now testing different directed search algorithms, of volume order 10^{19} or less. This will cut the search time from one day to about one hour, with much less chance of actuator failure.

Keywords: Telescope phasing, Aperture masking, Sparse telescopes, Space telescopes

1. Introduction

A deployable sparse space telescope can achieve high resolution, while maintaining minimal weight and volume for launch. An operational issue is the best way such a telescope can align

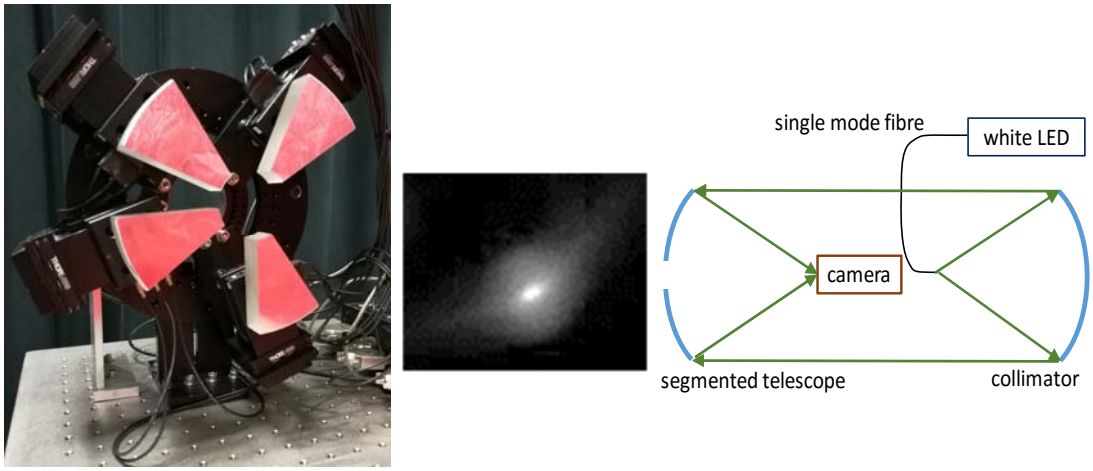

Figure 1. Laboratory experiment. Left: A 200 mm Cassegrain segmented sparse telescope (surface reflection from pink packaging material). Each segment has three degrees of freedom. Centre: The focal image of one of the segments, highly magnified. Notice the two long spokes stretching from the centre of the image, and the two broad ones at the other directions. As the other PSFs show different spokes directions, they are easily identifiable. Right: The optical set up.

itself in space to optical quality, while starting from a deployment accuracy, say 1mm, to reach 50nm surface errors. In previous laboratory studies we were able to avoid auxiliary metrology such as a wave front sensor, by maximizing the sharpness of the focal image [1-8]. Along the way, we realized that while it is possible to achieve such a fit within about one day by using random optimization (simulated annealing), it requires many trial movements of the 16 segments' actuators, heavily taxing their reliability.

Thus, we began searching for a faster converging method, with fewer calls to the actuators. Previous segmented telescopes provided a good guide, even if of contiguous segments. Since our aim is a simpler, smaller, and less expensive telescope, we chose to exploit the sparseness of the segments. We placed the four mirror sectors at non-redundant angles around the center. This identifies their unique PSFs in the focal plane and provides an error signal to correct their tip and tilt to the center of the field. Segment phasing is achieved by focusing one element while keeping the others still. As we identify the fringes between the reference segment and each other one, we are also able to reach optical path difference below a wavelength.

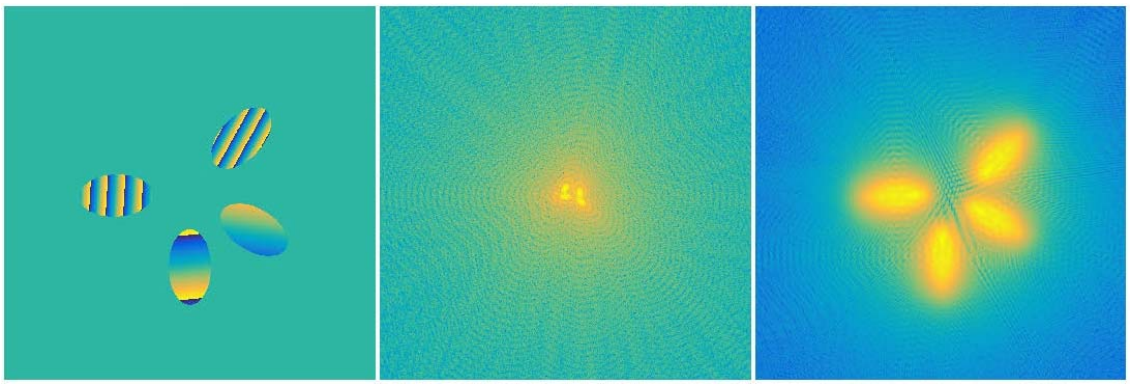

Figure 2. Left: tilted simulated elliptical panels. Centre: overlapped PSFs in the focal plane. Right: Defocused image, allowing segment identification and tilt calculation.

2. **Sector identification**

We cut four equal segments off a 200 mm parabolic f/6 mirror (Figure 1), and mounted each on a piezoelectric stage permitting tip, tilt and piston. Because of the limited travel we added coarse motors to the piston direction (total of 16 degrees of freedom).

The next issue was identifying the sector PSFs in order to correct for their tips and tilts. When they all have the same shape (e.g. hexagon), the common solution is to tilt them out and back in the camera. Here we can take advantage of their unique shapes, which lead to unique PSFs (Figure 1, right). In the case that they overlap in the focal plane, a known defocus removes the redundancy (Figure 2).

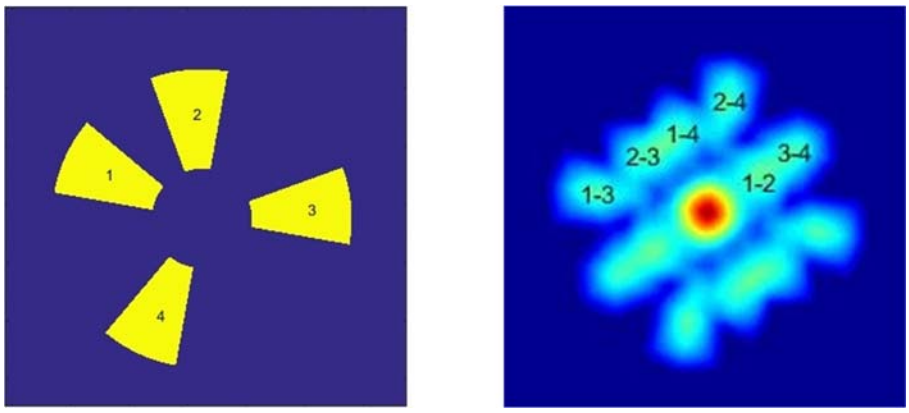

Figure 3. Model of the segments (rotated, left) and their mutual transfer function (right). Since the MTF is the autocorrelation function of the aperture, the segments were spaced so that their autocorrelations, where fringes appear, are not redundant: see their numbering identifications (the numbers are only marked in one half of the symmetric MTF).

3. **Pair identification**

Since the orientations of the sectors were chosen to avoid angular redundancy [5], each pair of sectors has a unique location in the autocorrelation of the whole aperture (Figure 3). This autocorrelation (the MTF) is the Fourier transform of the PSF and does not change with any of the degrees of freedom of the segments, which are all normal to the aperture plane. Thus the phase of each of the marked patches in Figure 3 represents directly the phase difference between the two corresponding sectors.

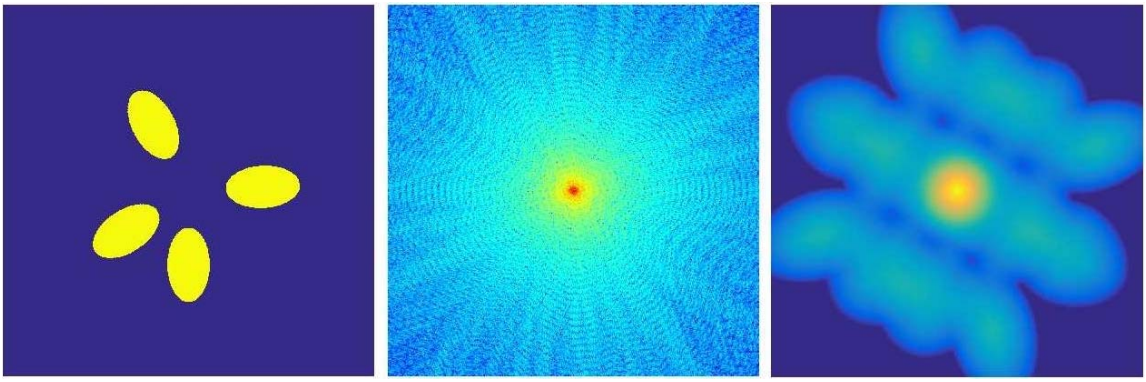

Figure 4. Four elliptical segments, their combined PSF, and their MTF (left to right). The angular placement of the sectors was optimised to obtain the smoothest MTF, while making sure that each sector pair (and their corresponding fringes) appear at different locations [5].

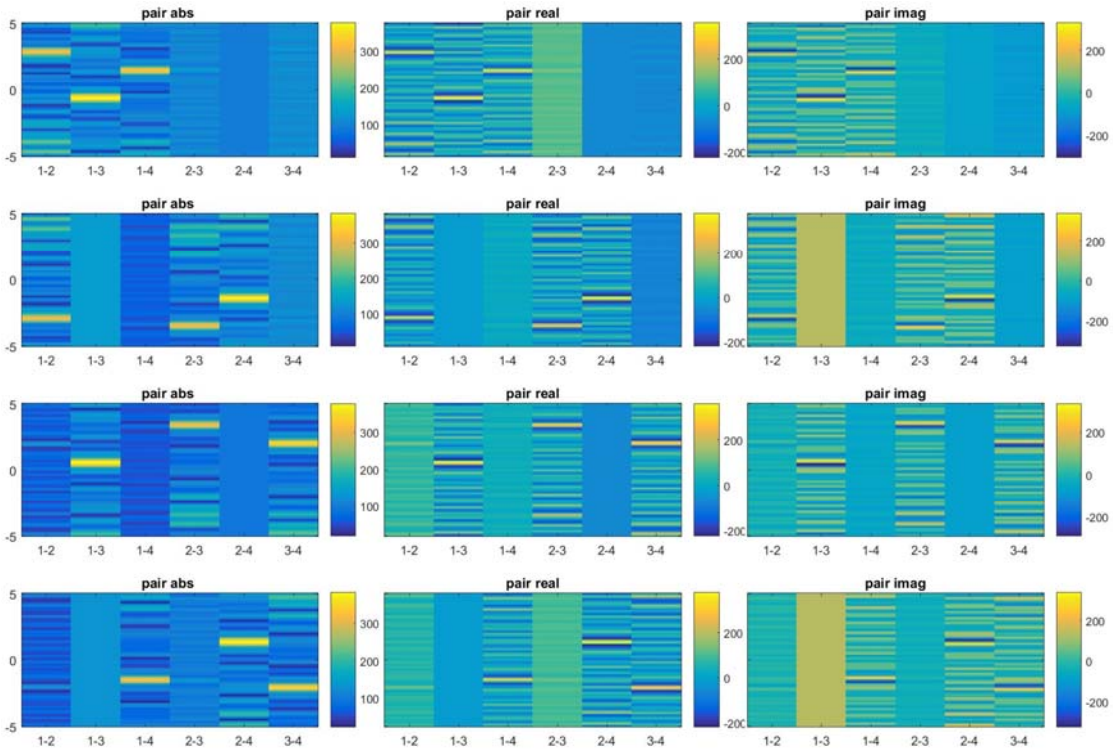

Figure 5. By moving each of the four segments by ±5 mm, and measuring the fringes with all the other segments, we can easily identify the central, white-light fringe (left column). More accuracy can be had from the real and imaginary parts of the fringes (centre and right columns). Notice that this is a redundant measurement, and moving only one element with respect to all others is sufficient (even if somewhat less accurate).

4. **Simulation**

After the successful identification, we continue with the hardware model, and at the same time develop a software model. Here we switch to a less scattering shape of sectors – elliptical ones [5]. We optimised their shapes and non-redundant spacings to get the flattest and widest MTF and we show one example here (Figure 4).

5. **Phasing**

Once we identify each fringe pattern with its pair of parent segments, we can scan the segments, one by one, and find the central white-light fringe. These positions are accurate to ~0.2λ and allow moving the segments to the best position. Final, but minimal, tip, tilt and defocus corrections optimise the sharpness down to the ultimate image [1-4]. Being near the solution allows using directed search rather than the slower stochastic one. The estimated reduction of the total search volume is at least ~10^{32}. The search time is reduced from ~1 day to ~1 hour, and actuator failure chances are negligible.

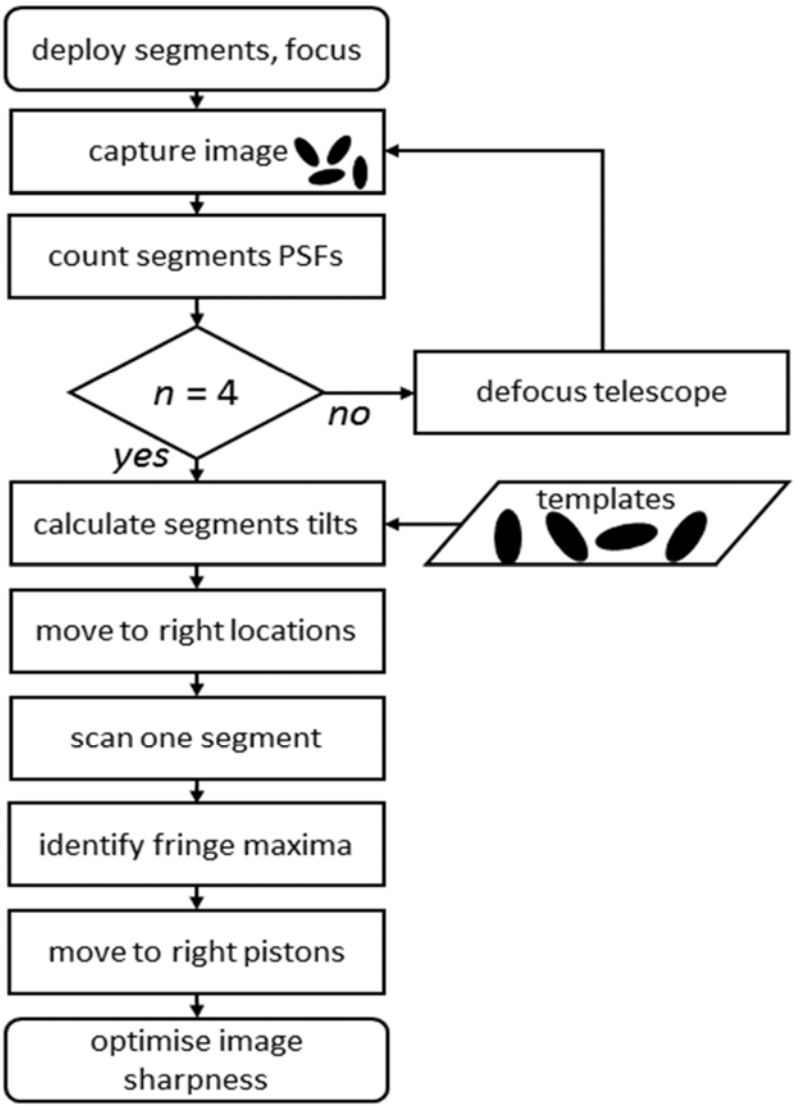

Figure 6. Process flow. First the telescope is focused, and all segments are identified in the focal image (either by wobbling them or correlating them with their templates). If they overlap, they can be separated by a known defocus. Then one segment is scanned against all others, to identify their mutual phase difference. Finally, they are all phased together, and optimised for the best image.

5. **Conclusions**

We showed that using only the degrees of freedom of the segments, and the focal image, it is possible to take a deployed sparse space telescope and align it to the best possible image.

Slower but safer simulated annealing search, with heavy actuator activity load, is replaced by a much faster directed search.

Parts of this research were supported by the Israeli Ministry of Science.

References

[1] N Brosch, V Balabanov and E Behar, Ultraviolet astronomy with small space. *Astrophysics and Space Science* **354,** 205-9 (2014).

[2] I Surdej, N Yaitskova, and F Gonte, On-sky performance of the Zernike phase contrast sensor for the phasing of segmented telescopes. *Appl. Opt.* **49**, 4052-62 (2010).

[3] R A Muller and A Buffington, Real-time correction of atmospherically degraded telescope images through image sharpening. *J. Opt. Soc. Am.* **64,** 1200-10 (1974)

[4] J P Hamaker, J D O'Sullivan, and J E Noordam, Image sharpness, Fourier optics, and redundant-spacing interferometry, *J. Opt. Soc. Am.* **67**, 1122-3 (1977).

[5] M J Booth, D Débarre, and T Wilson, Image-based wavefront sensorless adaptive optics. *Advanced Wavefront Control: Methods, Devices, and Applications V*, *SPIE* **6711**, 671102 (2007)

[6] D Dolkens, G Van Marrewijk and H Kuiper, Active correction system of a deployable telescope for Earth observation. *SPIE* **11180**, 111800A (2019)

[7] M. J. Golay, Point arrays having compact, nonredundant autocorrelations. J. Opt. Soc. Am. 64, 272-273 (1971)

[8] E N Ribak, B M Levine, Shaping apertures and masking, This meeting, paper SPIE 11446-79 (2020)